NF

NASA Technical Memorandum 82728
AIAA-81-2627

Low Speed Testing of the Inlets Designed for a Tandem-Fan V/STOL Nacelle

Robert C. Williams
Lewis Research Center
Cleveland, Ohio

and

Andres H. Ybarra
Vought Corporation
Dallas, Texas

Prepared for the
V/STOL Conference
cosponsored by the American Institute of Aeronautics
and Astronautics and NASA Ames Research Center
Palo Alto, California, December 7-9, 1981

NASA

LOW SPEED TESTING OF THE INLETS DESIGNED FOR A TANDEM-FAN V/STOL NACELLE

Robert C. Williams
National Aeronautics and Space Administration
Lewis Research Center
Cleveland, Ohio 44135

and

Andres H. Ybarra
Vought Corporation
Dallas, Texas 75265

Abstract

An approxmiately 0.25 scale model of a tandem fan nacelle, designed for a subsonic V/STOL aircraft, was tested in a Lewis wind tunnel. Model variables included long and short aft inlet cowls and the addition of exterior strakes to the short inlet cowl. Inlet pressure recoveries and distortion were measured at pitch angles to 40° and at combinations of pitch and yaw to 30°. Airspeeds covered a range to 135 knots (69 m/sec). The short aft inlet with added strakes had the best aerodynamic performance and is considered suitable for the intended V/STOL application.

Introduction

The military services are actively interested in the development of V/STOL aircraft. The Navy interest is centered around aircraft operations from smaller destroyer-sized ships and Air Force interest lies in operation from airfields with bombed or otherwise damaged airfields. There are also civilian applications for V/STOL aircraft including rescue missions, transportation into undeveloped areas and into city centers.

Three types of V/STOL aircraft can be identified: rotorcraft, subsonic cruise, and supersonic cruise. Each type of aircraft requires a propulsion system that can provide the thrust and the control of thrust needed for vertical takeoff and landing, the transition from engine supported to wing supported flight and conventional cruise. Many V/STOL airplane and propulsion concepts have been proposed and one such concept for a subsonic V/STOL aircraft proposed by the Vought Corporation uses the tandem fan propulsion system.

The proposed design for a subsonic V/STOL aircraft utilizing a tandem fan propulsion system is shown in figure 1. The figure illustrates a typical vertical landing sequence for the aircraft. During such a maneuver (and also during the takeoff) the aircraft must operate over a wide range of angles of attack and yaw at a variety of low airspeeds and the inlets must be designed to operate at these conditions. In addition, to those flight imposed inlet design requirements, the uniqueness of the tandem-fan propulsion system itself imposes some additonal design requirements on the inlet system. The description and the performance of the tandem fan inlet system over the required range of flight conditions; i.e., low speed at angles of attack and yaw, static, and cruise, is the subject of this paper.

Propulsion System Description

A schematic of the tandem fan propulsion system is shown in figure 2. In each of the two nacelles, two fans on a common shaft are driven by a single core engine. The front fan flow path is always independent of the flow path of the aft fan and core engine. An inlet and thrust deflecting nozzle system for each of the fans provides for a total of four thrust vectors that are directed vertically downward for takeoff and landing operations and directly aft for conventional flight.

Both of the inlets must be designed to provide good performance with minimum length. The front inlet must be kept short in order to improve crew side-visibility from the cockpit (see fig. 1). Its design is fairly conventional. The aft inlet must incorporate a short S-duct to deliver the airflow to the aft fan and engine core, while maintaining a minimum length of drive shaft to the front fan. An additional design constraint placed on the aft inlet is apparent from figure 2. The lower surface of the inlet must be designed to accomodate the gearbox that is used to interconnect all four fans to provide safe operation with one core engine failed.

Model Description

The approximately quarter size test model, designed and constructed by Vought, is shown in figure 3, installed in the LeRC 10- by 10- foot (3.05 m x 3.05 m) wind-tunnel.

The model was constructed of steel, aluminum, wood, and fiberglass, and is powered by a pair of 12 inch (30.5 cm) diameter fans driven by warm air powered tip turbines. The model fan performance approximates that of the full scale fan, with a pressure ratio of 1.4 at a fan face Mach number of 0.6, resulting in a corrected air flow rate of over 40 lb/sec/ft^2 (195 kg/sec/m^2). Fan speed was controllable, to simulate reduced thrust operations.

In addition to the "long" aft inlet shown in figures 1 to 3. A "short" inlet, shown, in figure 4 was also investigated as well as several modifications to this inlet which are presented later. Details of the inlet designs are given in references 1 and 2.

Results

Detailed test results for the aft and front inlet are also presented in references 1 and 2. The front inlet was relatively conventional in design and performance and is not discussed

herein. The present discussion deals with the more unique and difficult problem of the aft inlet, at static, low speed, and cruise flight conditions. The low speed results are discussed first.

Low Speed Conditions

The low speed conditions are those representing the transition from engine supported to wing supported flight that occur during takeoff and landing. Results are presented here for a typical low speed fight velocity of 135 knots (69 m/sec).

Angle of attack. Figure 5 presents steady-state values of pressure recovery and distortion as measured by the fan face rakes at angles of attack from -10° to +40 degrees, which represents a range greater than required for airplane operations.

The short inlet shows superior performance at low angles of attack, in terms of better pressure recovery and lower distortion. As a general rule, distortion values below 10 percent are acceptable. Consequently, the short inlet had unacceptable distortion values above a 20° angle of attack. The long inlet had acceptable distortion over the full range of angle of attack. Only gust conditions would cause angle-of-attack to 40 degrees.

Fan face isobar plots are shown in figure 6 for angles of attack of 0° and 40°. The numerical value of the pressure, expressed as a percentage of freestream total pressure, is printed adjacent to each isobar contour. Overall pressure recovery is printed in the center of each plot and steady total pressure distortion values are designated by "D".

Insight into the total pressure losses for each inlet can be gained by inspection of these plots. The long inlet loss pattern remains similar with increasing angle of attack. Losses are apparently from the inlet corners where the cowl joins the nacelle. (Similar results for a scarf inlet were reported in ref. 5). The excellent performance of the short inlet at zero degrees angle of attack is apparent from the lower left plot. At high angle of attack , the loss pattern extends to nearly the top of the fan face and is not obviously related to the inlet corners. The plots substantiate the conclusion of the previous figure that the short inlet, has excellent performance at low angle of attack but has degraded performance at high angles.

Static pressure taps located circumferentially around the lip leading edge were used to locate regions of high velocity. Results are shown in figure 7, which plots local static pressure, p, as a fraction of the freestream total pressure, P_{t_0}, as a function of lip circumferential location. During high angle of attack conditions, both inlets show high velocity (low static pressure) at the inlet corners. The deceleration from these high velocities to the velocity at the fan face and the related adverse pressure gradient could initiate internal flow separation in the inlet in a process similar to leading-edge stall of a thin wing. These curves support the idea that the corner region can be a problem.

In order to investigate this phenomena further, flow vizualization tests were conducted to study the corners of the short inlet at high angle of attack. A paint streak photograph from this investigation is shown in figure 8 for the short inlet at an angle of attack of 40°. This method of flow visualization is useful not only to indicate surface flow direction, but also reveals areas of separated flow. A surface liquid, such as the viscous paint used here, cannot flow from attached into separated flow because of flow reversal at the surface.

The paint pattern of this and similar photographs confirms that the origin of the flow separation is the inlet corner. Reverse flow is visible just inside the corner. A separated flow region proceeds downstream to nearly the top of the aft fan. Flow at the upper part of the side lips appears well attached. The tufts shown provided flow visualization at a wide variety of test conditions. Patterns of activity were recorded on videotape, and revealed that part of the flow that went into the inlet passed upwards along the side of the nacelle. (The tufts shown in the photograph are not in the actual position they were during the test, since the photograph was taken after the test was completed).

As a result of the flow analysis presented up to this point, several modifications were incorporated into the short inlet model in an effort to improve its performance at high angles of attack. First, filets were installed near the inlet corners to reduce velocity, but these proved to be ineffective. Next, sheet metal "strakes" were installed on the model as shown in figure 9 and found to be effective. The strakes are sheet-metal triangles, 15 cm wide by 36 cm long, and were installed about 5 cm below the corners of the short aft inlet.

The result of installing the strakes on the short aft inlet is shown by the paint streak photograph of figure 10. The figure reveals the improved flow inside the inlet corners. The strakes blocked the crossflow passing upwards along the sides of the nacelle and into the inlet corners. In addition, the vortex sheets from the strake leading edge helped to turn the flow into the inlet. The strakes have eliminated or reduced the flow separation at the corners of the short inlet. This conclusion is comparable to the findings in reference 4, which also discusses the beneficial effect of strakes. Also evident in the photograph is a vortex pattern on the external nacelle surface just downstream of the strake. This photograph, and a preceeding paint streak photograph, were taken originally in color, using a variety of paint colors. The technique is simple, informative, and a valuable adjunct to a formal wind-tunnel test program. The data in figure 11 show that the strakes have improved the inflow to the inlet. The regions of low total pressure have moved toward the bottom of the inlet. The magnitude of the separation has been reduced as is apparent from the increase in pressure recovery but some flow separation evidently still remains. Refinements in strake and inlet design might yield further improvements in inlet performance.

A summary of low speed inlet performance over a range of angle of attack is shown in figure 12.

At angle of attack of 40°, the short aft inlet with strakes has the highest pressure recovery and lowest distortion. At lower angles of attack this same inlet has acceptable distortion with high pressure recovery.

Combined angle of attack and yaw. Reference 4 discusses the effects of pitch and yaw on the performance of an aft inlet and indicates that combined angle of attack and yaw conditions can be more severe than either one individually. Therefore, inlet tests were conducted with the angle of attack, α, and the yaw angle, ψ, of equal value over a range from 0° to 30°. An isobar plot comparison of the three inlet configurations is shown in figure 13 for $\alpha = \psi = 30°$. On the figure, the arrows labeled V_0 show the direction of the free stream velocity vector. The data indicate that for each of the inlet configurations the losses are from the upwind inlet corner. The downwind corners show no total pressure losses. The short inlet again shows the loss pattern displaced circumferentially from the initial flow-separation, which starts at the upwind corner. The performance of the short inlet with strakes is again superior to that of the short inlet without strakes, and is also superior to the long inlet.

Static Conditions

A unique requirement for V/STOL aircraft inlets is good performance at the static conditions that are a part of takeoff, landing and hover. Typically, a 1 percent loss in pressure recovery can result in a 3 percent loss in thrust and a 15 percent loss in lift off payload. Figure 14 shows typical inlet performance and isobar plots at static conditions. The distortion pattern for the long aft inlet is similar to those shown previously at low speed conditions with losses originating at the inlet corners. The total pressure loss is about 1 percent. The short aft inlet has no measureable losses. The addition of the strakes to the short inlet is insignificant to its static performance.

Cruise Conditions

A subsonic V/STOL aircraft may cruise at a flight Mach number of 0.8 with the inlet at near zero degrees angle of attack. Because the maximum subsonic wind tunnel Mach number is 0.36, cruise inlet flow conditions were simulated by duplicating the inlet freestream to fan face velocity ratio. Matching this velocity ratio reproduces the cruise flow streamlines (except for compressibility effects) and provides a method for estimating cruise performance from low speed test conditions. (At low speed conditions, the capture streamtube is larger than the inlet leading edge area (or $V_0/V_{LE} < 1$) but at cruise conditions the capture streamtube is generally smaller than the inlet leading edge area ($V_0/V_{LE} > 1$). In both cases the peak inlet surface velocities occur at the inlet leading edges or highlight).

Figure 15 presents the circumferential variation of local surface Mach number at the inlet leading edge at the simulated cruise conditions described above. On the left hand ordinate the experimentally measured leading edge Mach number is shown at a freestream Mach number of 0.36. The right hand ordinate present the values of leading edge Mach number scaled up to a freestream Mach number of 0.8. It is desirable to keep the peak Mach number low in order to avoid the drag increases that may occur from external lip flow separations. Separation can occur if the peak Mach number gets high enough to induce a shock of significant strength ($M_{LE} > 1.4$) or the velocity ratio over which the flow must diffuse becomes excessive ($M_{LE}/M_0 > 2$).

Based on these separation criteria, the results shown in figure 15 indicate that both inlets would have attached external flow at cruise. Comparing the two inlets, it is seen that the long aft inlet has the higher peak Mach number, point A, and it occurs in the corner. The short inlet's maximum peak Mach number, point B, occurs at the top of the inlet. Hence, the short inlet with its lower peak Mach number would be expected to have ahigher drag-rise Mach number than the long inlet.

It should be noted, however, that the estimates presented by the right hand ordinate do not account for compressibility. If compressibility had been accounted for, the peak Mach numbers for both inlets would be higher and the cruise performance of this long aft inlet configuration could be marginal and require redesign of the inlet lip contours.

Summary of Results

From a comparison of the performance of the long and short aft inlet configurations, the following conclusions can be drawn:

1. The short inlet has better low speed performance at angles of attack from -10° to +10°.

2. With strakes added, the short inlet also gives the best performance at low speeds for angles of attack from 10° to 40° and for combined angles of attack and yaw up to 30° each.

3. At static conditions, the pressure recovery of the short inlet is nearly 100 percent, which is 1 percent higher than the long inlet recovery.

4. At cruise conditions, the short inlet has lower peak surface Mach numbers than the long inlet and would be expected to have a higher drag-rise Mach number.

References

1. Rhoades, W. W. and Ybarra, A. H., "Low Speed Test of the Aft Inlet Designed for a Tandem Fan V/STOL Nacelle," NASA CR-159752, Feb. 1980.

2. Ybbarra, A. H., "Additional Testing of the Inlets Designed for a Tandem Fan V/STOL Nacelle," NASA CR-165310, June 1981.

3. Ybarra, A. H. and Williams, R. C., "Low Speed Test of the Aft Inlet Designed for a Tandem Fan V/STOL Nacelle," AIAA Paper 80-1247, July 1980.

4. Widing, K., "A Study of the Inlet Efficiency of a Combat Aircraft Concept with Dorsal Inlet," International Council of the Aeronautical Sciences, Congress, 13th, Munich, West Germany, October 12-17, 1980, Proceedings, AIAA, pp. 173-182.

5. Abbott, J. M., "Aerodynamic Performance of Scarf Inlets," AIAA Paper 79-0380, Jan. 1979.

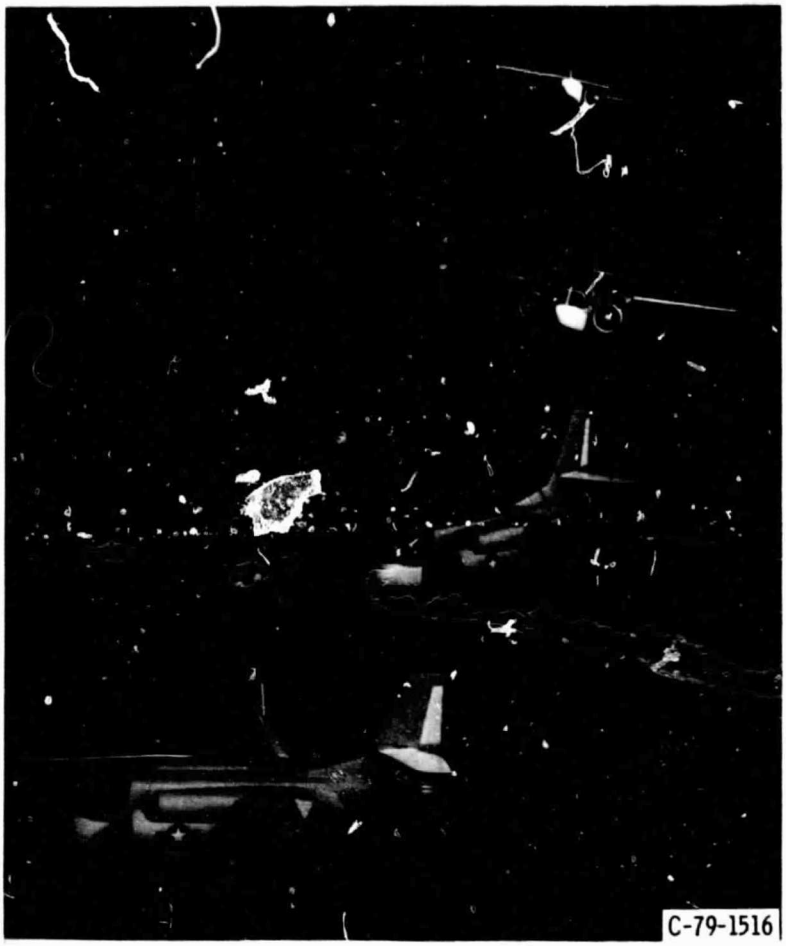

Figure 1. - Proposed tandem-fan V/STOL aircraft.

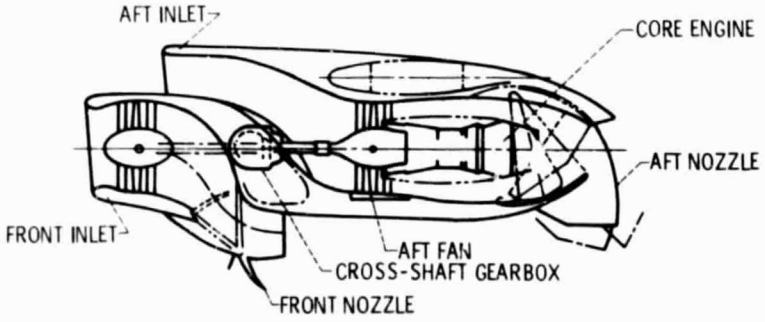

Figure 2. - Schematic of tandem-fan nacelle.

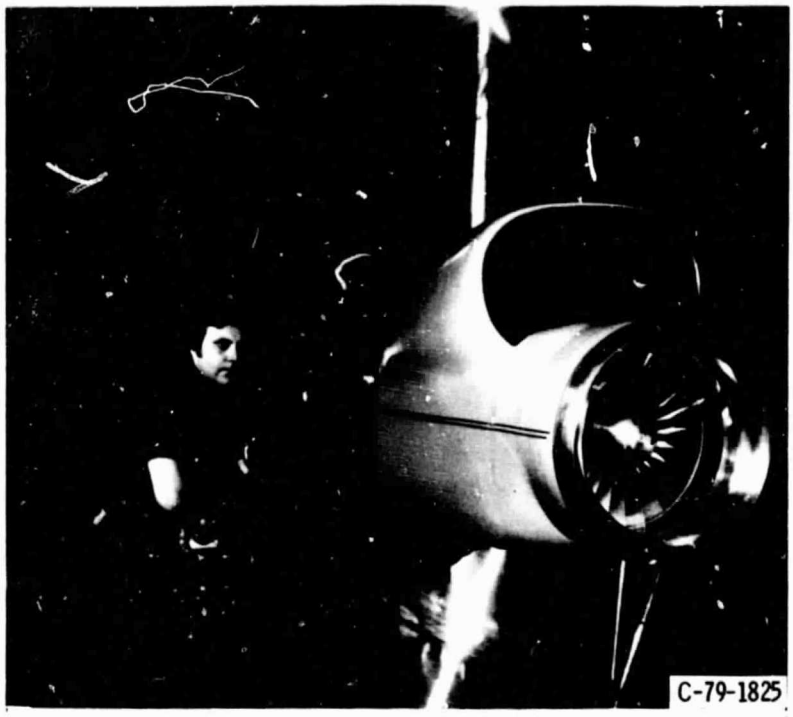

Figure 3. - Long aft inlet model installed in Lewis wind tunnel.

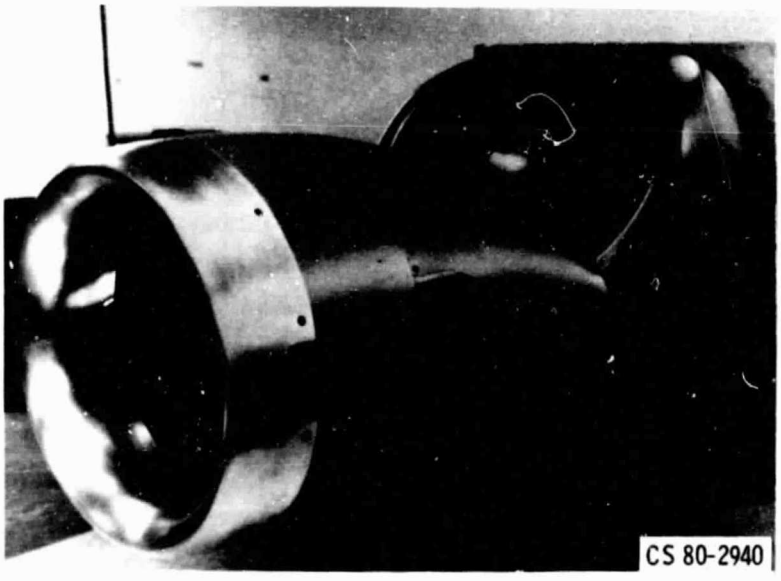

Figure 4. - Short aft inlet.

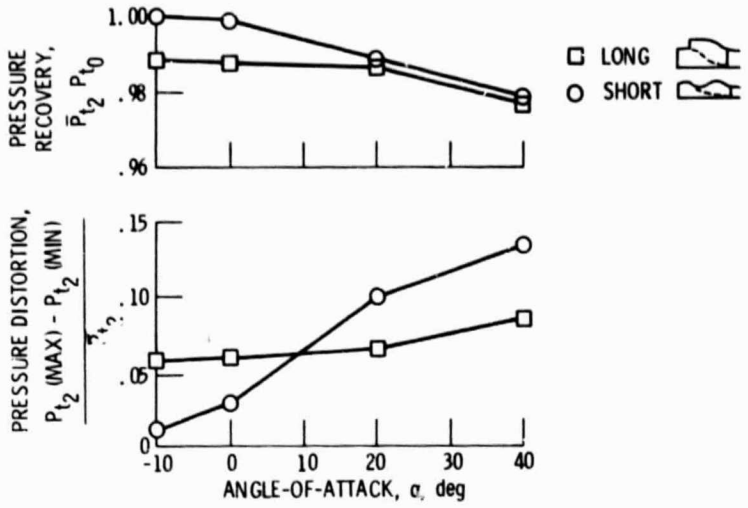

Figure 5. - Comparison of aft inlet performance. V_0 = 135 knots (69 m/sec), both fans at full rpm.

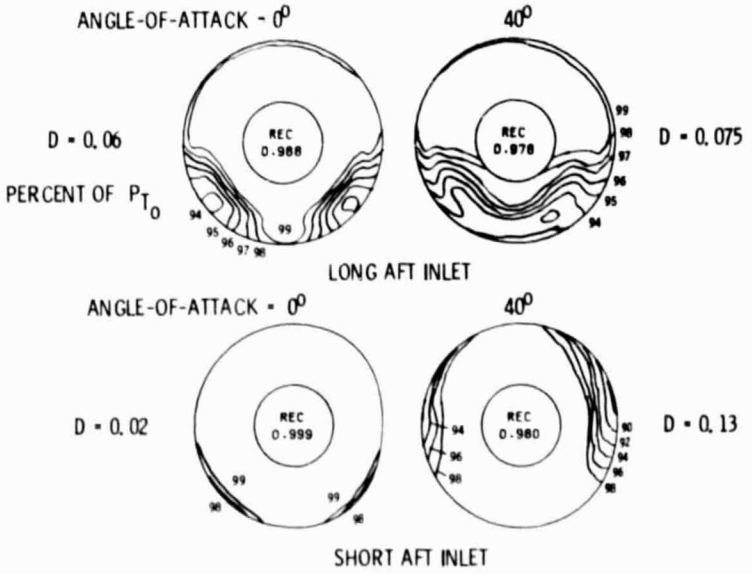

Figure 6. - Aft inlet total pressure isobars. V_0 = 135 knots (69 m/sec), both fans at full rpm.

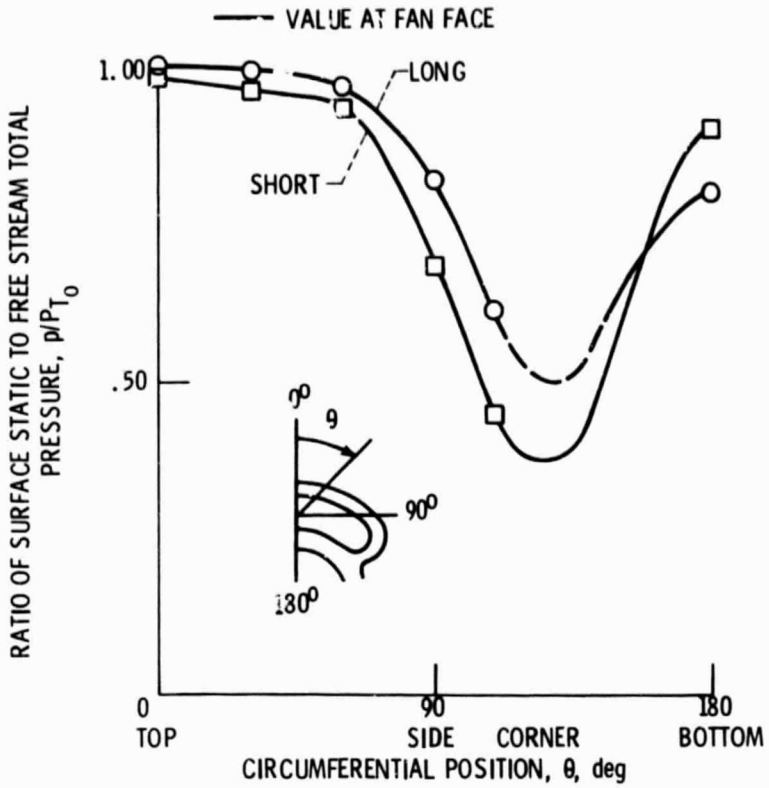

Figure 7. - Aft inlet surface static pressures at lip leading edge. V_0 = 135 knots (69 m/sec), $\alpha = 40^0$, both fans at full rpm.

Figure 8. - Short aft inlet paint streak pattern. V_0 = 80 knots (41 m/sec), $\alpha = 40^0$, both fans full rpm.

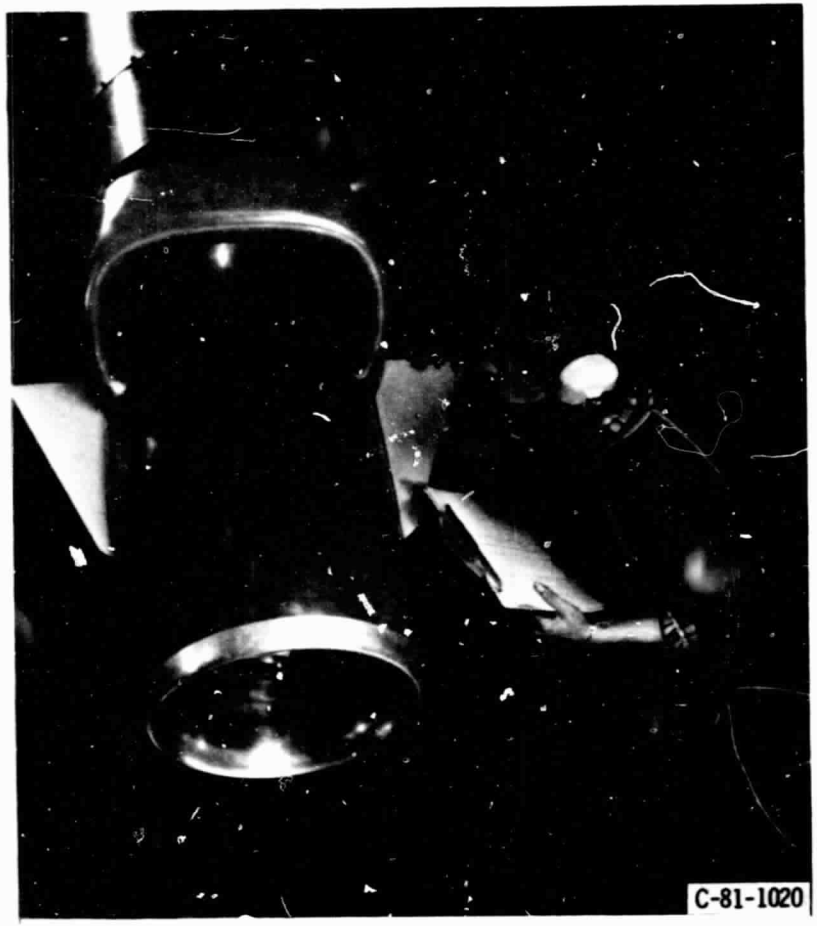

Figure 9. - Short aft inlet with strakes.

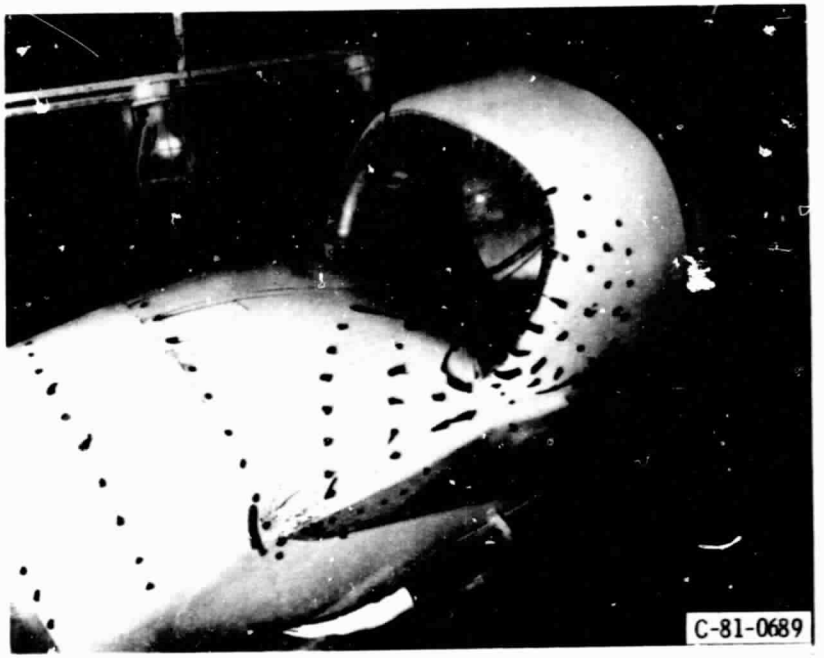

Figure 10. - Short aft inlet with strakes, paint streak pattern, V_0 = 80 knots (41 m/sec), $\alpha = 40^0$, both fans full rpm.

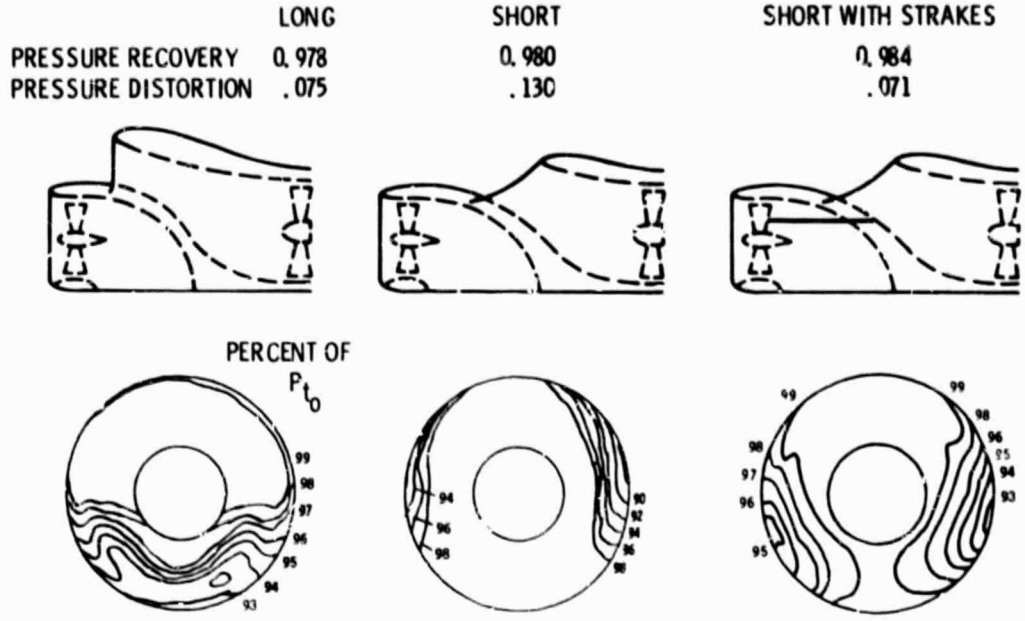

Figure 11. - Aft inlet total pressure isobars, $\alpha = 40^0$, $V_0 = 135$ knots (69 m/sec), both fans at full rpm.

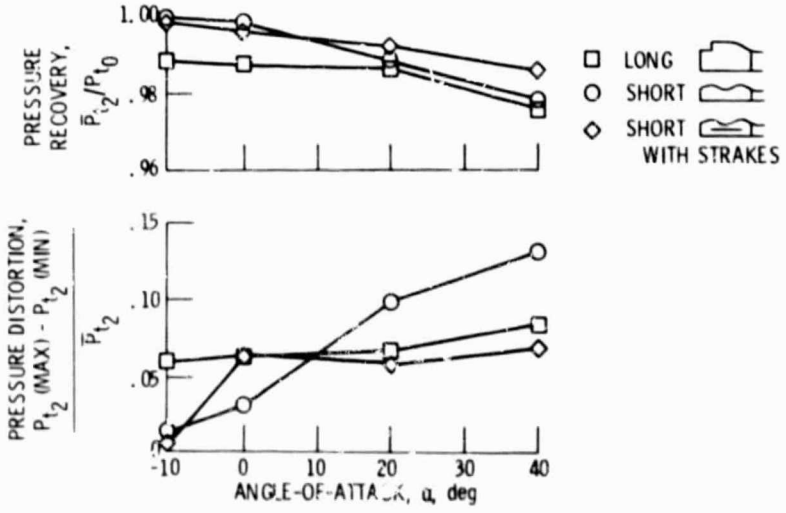

Figure 12. - Comparison of aft inlet performance, $V_0 = 135$ knots, (69 m/sec), both fans at full rpm.

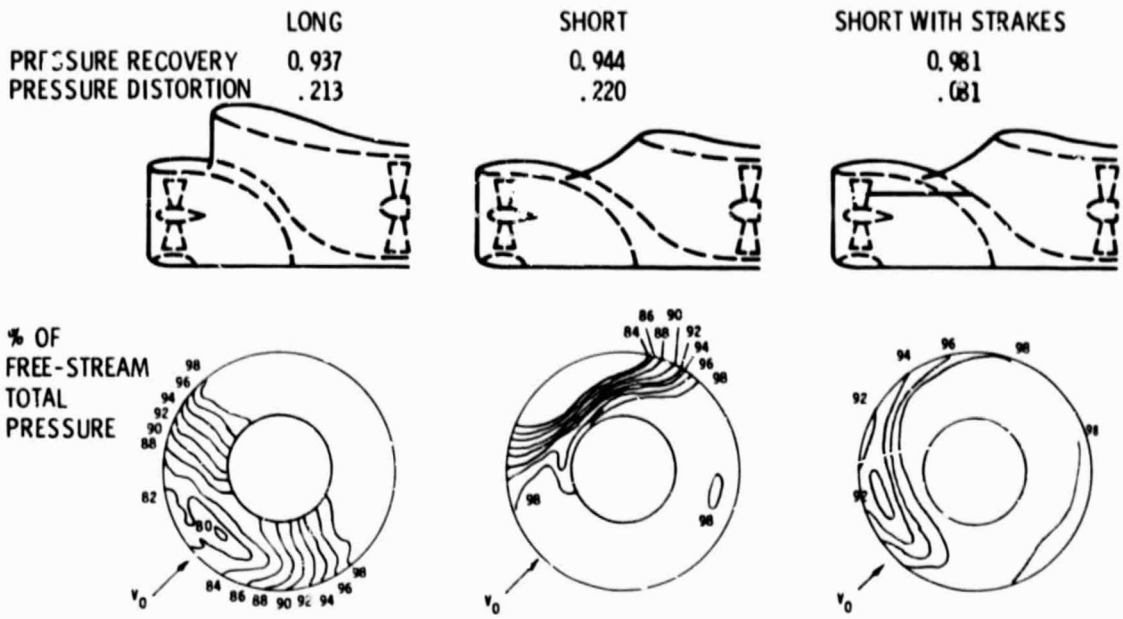

Figure 13. - Aft inlet total pressure isobars, $\alpha = \psi = 30^0$. V_0 = 135 knots (69 m/sec), both fans at full rpm.

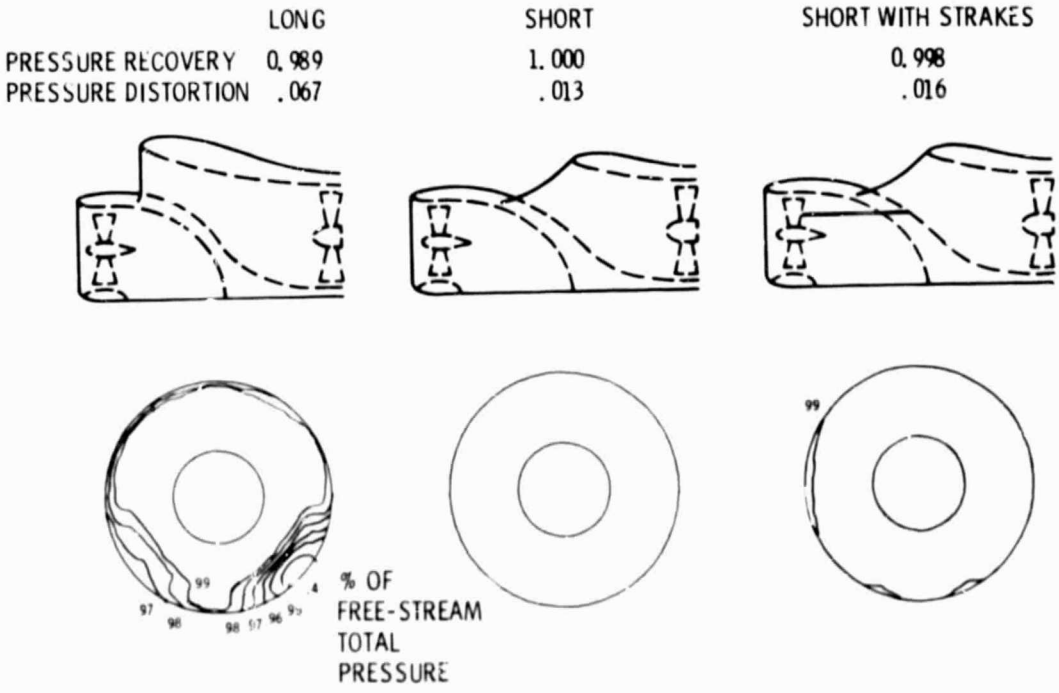

Figure 14. - Aft inlet total pressure isobars, V_0 = 0, both fans at full rpm.

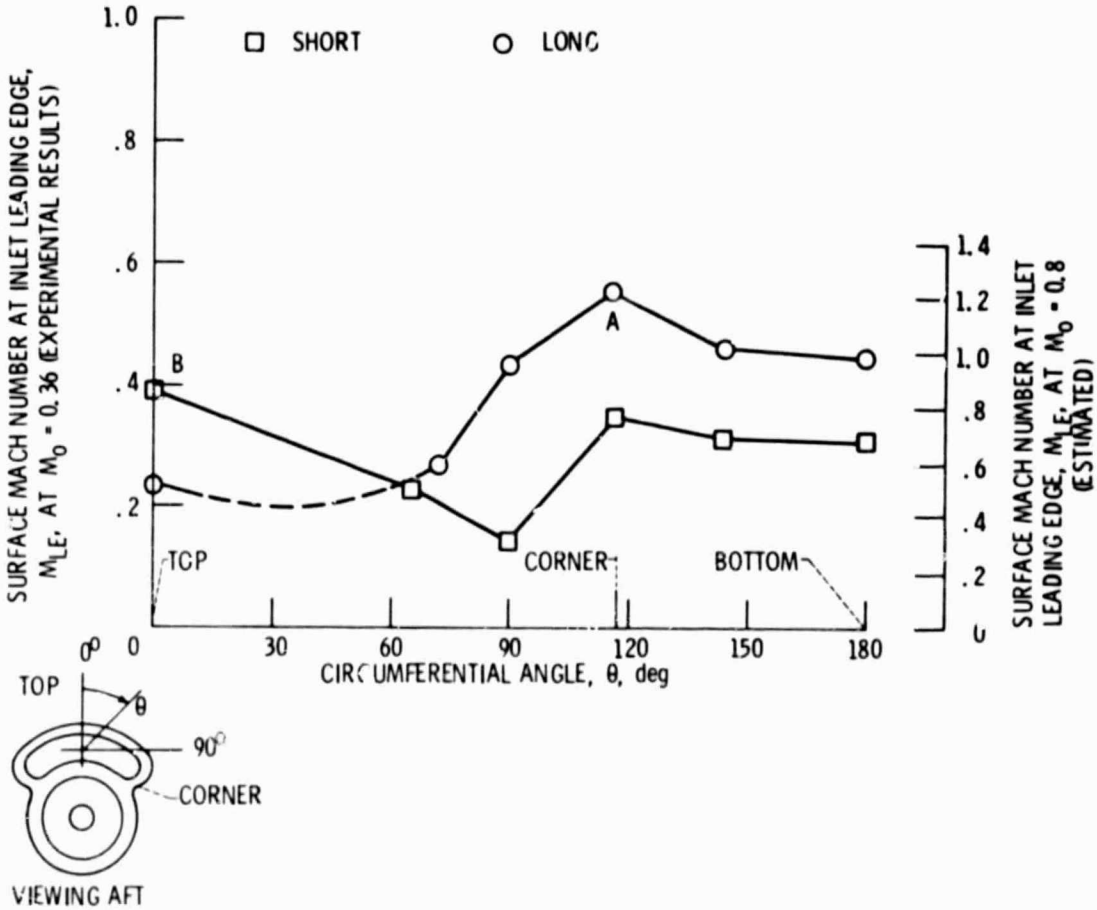

Figure 15. - Comparison of aft inlets at cruise velocity ratio M_{FF}/M_0 = 0.5/0.8.